Journal of Physics Research and Education, Volume 3, March 2026

On the Ferroelectricity in $CaBaCo_{3.96}Ni_{0.04}O_7$

Mijanul Islam and Arindam Karmakar*
Department of Physics, Surya Sen Mahavidyalaya, Siliguri 734 004, India

Studies over the last decade demonstrate a large electric polarization and a substantial ferrimagnetic moment in $CaBaCo_4O_7$. The robust polarization, produced along the crystallographic c-direction, is however recently found to be a result of pyroelectricity rather than switchable polarization as in ferroelectricity. A contemporary investigation of lightly Ni-doped $CaBaCo_4O_7$ derivatives claims switchable polarization indicating ferroelectricity in the materials. In an attempt to delve deeper into the debate, we have attempted direct $P(E)$ loop measurements of two compounds as a comparison–a 1% Cr-doped (trivalent) and a 1% Ni-doped (divalent) $CaBaCo_4O_7$ derivative. The Ni-doped compound shows ferroelectric-like $P(E)$ loops while the Cr-doped compound does not. We have also discussed the possible origin of the switchability of the polarization from the perspective of structural distortion and argued that a possible candidate is the buckling of the CoO_4 tetrahedra rather than the cooperative orthorhombic distortion which only enhances the net pyroelectric polarization.

I. INTRODUCTION

The '114' transition metal oxide $CaBaCo_4O_7$ exhibits substantial ferrimagnetic moment [1] and gigantic electric polarization change ($\Delta P \approx 17$ mC-m^{-2}) along the crystallographic c-direction [2], originating as a result of structural distortion [1, 3] and mediated via magnetostriction. The material gained a lot of attention in the last decade for having the potential of technological applications in gas sensor, pyroelectric sensors, magnetocaloric devices, etc. Not only that, but the two-dimensional layered structure of the Co-network, the inherent geometrical frustration in the kagomé patterns of the Co-ions, the magnetoelectric coupling, and the innate competing magnetic interactions giving rise to a non-collinear zig-zag spin order also make the material an ideal playground for fundamental study of the interplay of structure, magnetism, and polarization. A primary focus of recent research in the system is tuning physical properties through chemical substitution. It has been reported that trivalent dopants such as Cr^{3+} and Fe^{3+} occupy the triangular layer or specific kagomé sites without significantly altering the polar nature. Contrarily, a different nature is observed due to divalent Ni^{2+} doping; for example, a four-fold enhancement in electric polarization is observed in 1% Ni-doped compound compared to insignificant changes in 1% Cr-doped compound [4].

Single crystal studies of $CaBaCo_4O_7$ showed that the polarization was not switchable upon reversing the electric field [2] and the material was later argued to be a ferrimagnetic pyroelectric [5]. However, a later study of Ni-doped derivatives of $CaBaCo_4O_7$ claimed ferroelectric properties based on the observation of switchable polarization, as demonstrated using different pyroelectric current measurement protocols. In this article, we present a direct evidence of ferroelectricity in an impurity level 1% Ni-doped compound $CaBaCo_{3.96}Ni_{0.04}O_7$ through the observation of isothermal

* akarmakar@suryasencollege.org.in

ferroelectric-like polarization [$P(E)$] loops. As a comparison, the absence of similar isothermal $P(E)$ loops has also been demonstrated for a 1% Cr-doped $CaBaCo_{3.96}Cr_{0.04}O_7$. We further attempted to correlate the origin of the ferroelectricity with orthorhombic distortion, CoO_4 tetrahedral tilting, rotation and buckling using high-energy synchrotron x-ray powder diffraction analysis.

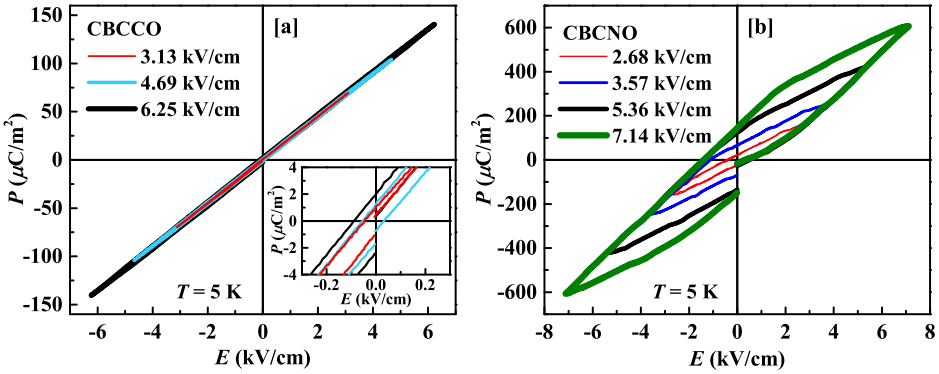

FIG. 1. Isothermal $P(E)$ loops at 5 K of (a) CBCCO and (b) CBCNO at different maximum electric fields. The inset in (a) highlights the region near the origin of $P(E)$ loops of CBCCO.

II. EXPERIMENTAL DETAILS

Polycrystalline samples of three compounds - the mother $CaBaCo_4O_7$ (CBCO), 1% Cr doped $CaBaCo_{3.96}Cr_{0.04}O_7$ (CBCCO) and 1% Ni doped $CaBaCo_{3.96}Ni_{0.04}O_7$ (CBCNO) were synthesized using standard solid state reaction method described in our earlier paper [4]. Correct synthesis and phase formation were checked by room temperature powder X-ray diffraction (PXRD) patterns recorded using Cu-K_α radiation ($\lambda = 1.5406$ $\mathring{A}$) in a Bruker D8-Advance X-ray powder diffractometer. Temperature-dependent high-energy PXRD data were collected in P21.1 beamline in PETRA III light source of DESY [6] using an energy of 101.46 keV ($\lambda = 0.1222$ $\mathring{A}$) and sample to detector distance of 1 m. Analysis of the PXRD data were done using `FullProf` software package [7] for in-depth structural studies. Isothermal polarization loops [$P(E)$] were obtained using Precision Premier II loop tracer from Radiant Technologies. For recording $P(E)$ loops, thin rectangular pieces of pellets, $\sim$ 0.3 - 0.6 mm in thickness, were used to fabricate parallel plate capacitors with the sample as the dielectric medium. Electrodes were painted on the faces using air-drying silver paint, which was baked at 200°C in a vacuum, prior to experiments.

III. RESULTS AND DISCUSSIONS

A. $P(E)$ loops

Figure 1 (a) and (b) show the $P(E)$ loops measured at a temperature (T) of 5 K for CBCCO and CBCNO, respectively. The inset in (a) highlights the central region of the graph near the origin. The loops of CBCCO are almost straight lines with nearly zero coercivity, representing

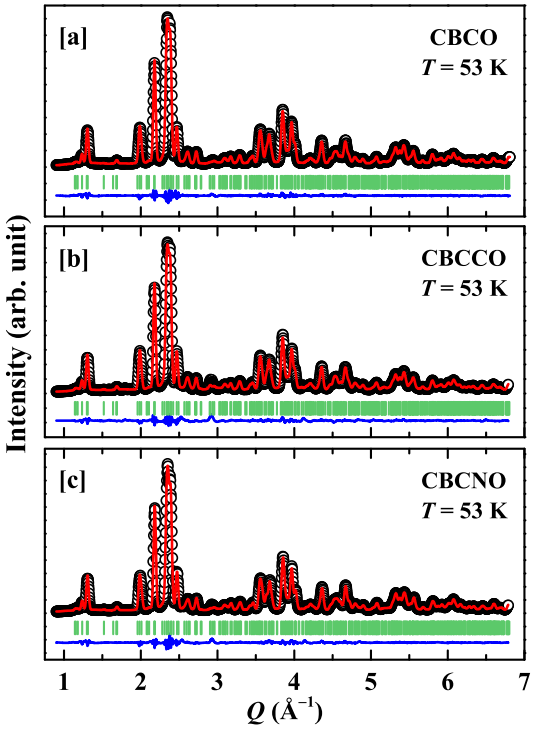

FIG. 2. Powder x-ray diffraction patterns and Rietveld refinement fits of (a) CBCO, (b) CBCCO, and (c) CBCNO at 53 K and with λ = 0.1222 $\AA$. Black symbols indicate the experimental data points, the red solid curves show the calculated diffraction patterns, the blue curves represent the difference plots, and the green markers denote the Bragg reflections. The goodness of fitting parameters obtained are $R_{wp} = 5.56\%$ and $\chi^2 = 2.23$ for CBCO, $R_{wp} = 5.23\%$ and $\chi^2 = 2.12$ for CBCCO, and $R_{wp} = 5.44\%$ and $\chi^2 = 2.04$ for CBCNO.

no switchable electric polarization (P). This can appear from a paraelectric, antiferroelectric or a non-ferroelectric pyroelectric material. As we obtained finite electric polarization change (ΔP) in a T-variation, measured and reported earlier, in a polycrystalline sample [4], the graphs in Fig. 1 (a) surely represent finite but non-switching P. Indeed, the mother CBCO reportedly exhibits non-switching but gigantic ΔP due to the non-ferroelectric pyroelectric nature of the compound [2, 5]. The slight coercivity observable in the inset in Fig. 1(a) is possibly the result of leakage current due to finite electrical conductivity—typically called a 'lossy' loop. CBCNO, however, exhibits loops with considerable coercivity (E_c), and a step-like change in either arm, indicating switching P, representing ferroelectric (FE) loops. The E_c increases with increasing maximum electric field ($E_{\max}$) up to 5.36 kV/cm, and thereafter it saturates. P however does not saturate even for $E_{\max}$ = 7.14 kV/cm. $E_{\max}$ could not be increased further due to the buildup of high leakage current.

B. Correlation with structural properties

X-ray powder diffraction patterns at 53 K are shown in Figs. 2(a), 2(b) and 2(c) for CBCO, CBCCO and CBCNO, respectively, along with the respective Rietveld refinement fits. The patterns

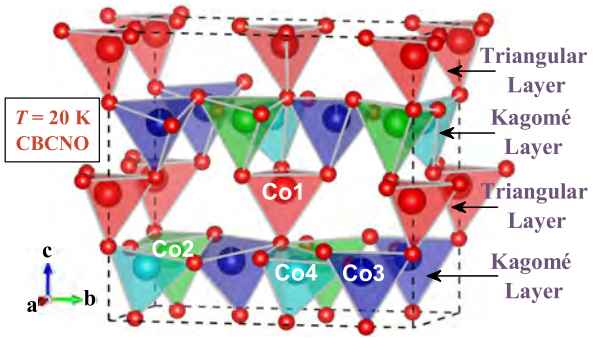

FIG. 3. A unit cell of the crystal structure of CBCNO at 20 K showing the two dimensional layered arrangement of the corner-sharing CoO_4 tetrahedra in the triangular and kagomé layers.

are fitted with orthorhombic $Pbn2_1$ space group. The fits are quite satisfactory, as obvious from the blue difference plots, as well as from the acceptable values of various refinement parameters given in the caption of the figure. The crystal structures of the materials exhibit an alternating stacking of two-dimensional layers with triangular and kagomé patterns of Co ions, encased in corner-sharing CoO_4 tetrahedra. The triangular layer is composed entirely of Co1 sites, whereas the kagomé layer contains Co2, Co3, and Co4 sites. A representative diagram of the crystal structure is shown in Fig. 3.

Investigations on CBCO to date indicate that the use of the smaller sized and divalent Ca-ions at the A site in CBCO leads to a robust orthorhombic distortion compared to the earlier compounds in the family, *viz.* RBaCo$_4$O$_7$ (R = Rare-earths or Y) [8–12], transforming the material from the $P6_3mc$ precursor hexagonal structure of the older compounds to the orthorhombic $Pbn2_1$ structure of CBCO. This relieves the geometrical frustration in the kagomé layers, producing a long-range ferrimagnetic order [1]. One can note that most of the earlier compounds exhibited short-range magnetic order and no electric order at all [9, 11, 13, 14]. The distortion consequently leads to a remarkable electric polarization change (ΔP), a non-ferroelectric pyroelectric effect, via magnetostriction in CBCO [3]. Precisely, this distortion leads to a relative tensile elongation along the b-axis and relative compression along the a-axis, distorting the ab-plane, which manifests mainly in terms of *tilting* and/or *rotation* of the CoO_4 tetrahedra.

A distortion parameter defined in orthorhombic systems is $\delta = |a - b|/(a + b)$ where a and b are the respective lattice parameters. δ quantifies the distortion in the ab-plane as the structure deviates from an ideal tetragonal one. For an ideal tetragonal structure $\delta = 0$. We have analyzed the high-energy X-ray powder diffraction profiles in the T-range of approximately 15 K $-$ 150 K for the three samples using Rietveld refinement procedures. δ for the three samples are shown in Fig. 4(a). The data show that CBCCO has a slightly lower δ than CBCO, while CBCNO has a significantly larger value. It is thus clear that Cr-doping reduces the orthorhombic distortion to some extent while Ni-doping enhances it strongly, in particular, a robust tensile elongation along the b-axis is evident in CBCNO leading to a larger tilting and/or rotation. Again, the extension or compression along the axial c-direction can be quantified by the ratio c/a, where c and a are the respective lattice parameters. The ratio is shown in Fig. 4(b) for the three samples. It is clear from the data that Cr-doping causes an extension along c while Ni leads to a significant compression. The orthorhombic distortion discussed above is a cooperative phenomena occurring in the entire crystal as a whole. However, it would be quite interesting also to investigate the local distortion of

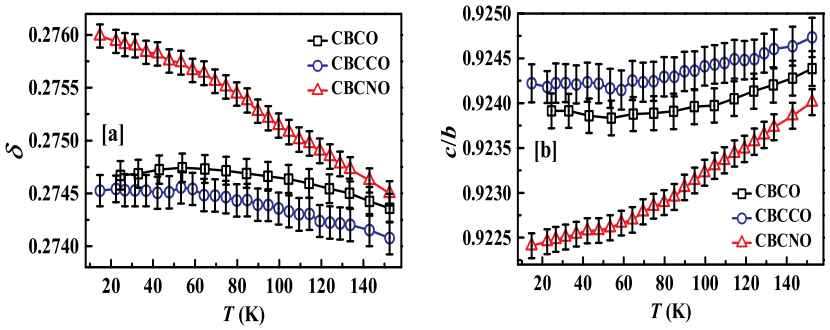

FIG. 4. Thermal variation of the (a) distortion parameter δ and (b) ratio c/a for the three samples between $\sim$ 15 and 150 K. (See text for definitions).

the CoO_4 tetrahedra.

The intra-tetrahedral picture relates a different story. We have probed the Co−O bond-splitting in the CoO_4 tetrahedra in the T-range 15 K − 150 K using standard deviation (σ) defined as

$$\sigma = \sqrt{\frac{1}{n}\sum_{i=1}^{n}(d_i - d_{\rm av})^2} \tag{1}$$

where d_i are the individual bond lengths in a CoO_4 tetrahedron, $d_{\rm av}$ is the average bond length in the tetrahedron and n is the total number of bonds in the tetrahedron (here $n = 4$). Figure 5 shows the T-dependence of σ in the CoO_4 tetrahedra at the four Co-sites as a comparison for the three samples. We are mainly interested in the T-range below $\sim$ 60 K which is near the ferrimagnetic T_c of the samples [4]. The bond-splitting indicates the degree of deviation of the Co−O bonds about its mean value, essentially indicating *buckling* of the tetrahedra. CBCCO shows considerably larger bond splitting at all Co-sites in the kagomé layer (namely Co2, Co3, and Co4) and practically minimal splitting in the triangular layer (Co1), compared to CBCO. Splitting in CBCNO remains modest and similar to CBCO at Co1, Co3 and Co4 sites but, interestingly, at the Co2-site it gradually reduces towards zero as cooled below 100 K up to $\sim$ 15 K. Thus overall the picture is that the 1% Cr-doping largely increases tetrahedral buckling while 1% Ni-doping reduces the distortion to nearly an ideal tetrahedron, particularly at the Co2-site. It may be noted that, as earlier studies indicate, Ni is mainly doped at the Co2 and the Co3 sites [4] while the magnetic ordering and the consequent electric order mediated via magnetostriction largely depends on the configuration of the kagomé layer, and so it should definitely depend on the CoO_4 tetrahedral distortion [1, 15].

IV. DISCUSSION AND CONCLUSIONS

The appearance of ferroelectricity in $CaBaCo_{3.9}Ni_{0.1}O_7$ (CBCNO1) was discussed in [15] by Dhanasekhar *et al.* using pyroelectric current measurements in different protocols, and the origin was investigated using neutron powder diffraction studies. In CBCO, the in-plane non-collinear spin arrangement of Co in the kagomé layer shows spins orienting towards, but not exactly to, the b-direction. Also, the spins are arranged in zig-zag chains running along the b-direction, with

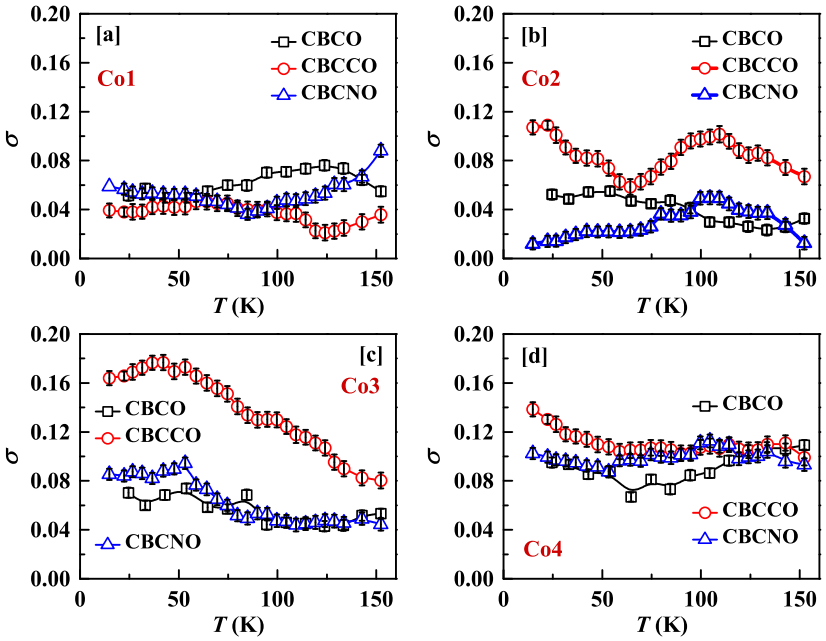

FIG. 5. Thermal variation of the standard deviation σ of bond-length splitting [Eq. (1)] at the (a) Co1, (b) Co2, (c) Co3 and (d) Co4 sites, respectively, for the three samples. In order to aid ready comparison of the data, the scales of the σ-axes are made the same in all four panels.

the Co1 spins in the triangular layer antiferromagnetically coupled to the triangular Co2-Co3-Co4 triad located just below it in the kagomé layer. Dhanasekhar *et al.* showed that in CBCNO1 this was transformed to an in-plane collinear spin arrangement of Co, pointing exactly along the a-direction, running along the same zig-zag chains in the b-direction as a consequence of weaker interlayer coupling due to an increase in the c/a ratio. The Co(Ni)2-Co(Ni)3-Co(Ni)2-Co(Ni)3 and Co(Ni)2-Co4-Co(Ni)2-Co4 spin quartets are arranged in the $\uparrow\uparrow\downarrow\downarrow$ type patterns in the zig-zag chains within the kagomé layer while a Co1 in the triangular layer couples antiferromagnetically with a ferromagnetically coupled ($\uparrow\uparrow\uparrow$) Co(Ni)2-Co(Ni)3-Co4 triad arranged in a triangle and located just below the Co1 in the kagomé layer. The investigation pointed out that the attempt to explain the origin of ferroelectricity from the perspectives of alternate long and short bonds between parallel ($\uparrow\uparrow$) and anti-parallel ($\uparrow\downarrow$) spins, respectively, along with respective shifts of oxygen, was not successful as alternate kagomé layers would then produce opposite electric polarization vectors $\boldsymbol{P}$ that would ultimately lead to antiferroelectricity rather than ferroelectricity. However, they pointed out that it could be realized if Ni is not substituted uniformly in all the kagomé layers so that the $\boldsymbol{P}$ is not equally canceled out in every consecutive kagomé layer.

Meanwhile, our investigation in this article provides more direct evidence of ferroelectricity using $P(E)$ loops. Moreover, we observed the appearance in a still lower Ni-doping concentration of 1% compared to the 2.5% sample discussed above [15]. The evidence of ferroelectricity in the lower doping percent (rather an impurity level doping) may support the argument of a non-uniform doping scenario where it is quite possible for Ni to segregate in isolated locations. On the other hand, our high energy PXRD analysis shows that Ni-doping significantly enhances the ab-plane orthorhombic distortion while reducing the c/a ratio (quite contrary to Dhanasekhar *et*

al. [15]) that leads to stronger tilting and rotation of the CoO_4 tetrahedra which may give rise to enhanced polarization (ΔP), in a manner similar to CBCO, which is a pyroelectric material with a non-switchable polarization along the c-direction. But this does not explain the switchability in the $P(E)$ loops, and the consequent ferroelectricity. Modulations in the local structural distortion of the CoO_4 tetrahedra, leading to bond splitting via buckling, may be another potential cause, as this scenario may give rise to locally switchable polarization via charge density separations. The reduction of the CoO_4 tetrahedral distortion, precisely at the Co2-site only, is quite unique for CBCNO, while the distortion at other sites remain similar to CBCO. This may give rise to the possibility of an unbalanced net ***P*** among the four Co-sites nearby. We propose further studies in this direction with still higher resolution PXRD and local probes like XAS, along with theoretical calculations.

Acknowledgements : M. Islam and A. Karmakar are grateful to Souvik Chatterjee, project co-ordinator at UGC-DAE-CSR Kolkata, for using extensive laboratory facilities. We also thank UGC-DAE-CSR for the financial support through the CRS projects CRS/2022-23/02/817 and UGC-DAE-CSR-KC/CRS/19/MS05/0936. We express our gratitude to Sanat K. Adhikari, UGC-DAE-CSR Kolkata, for technical support during measurements. We acknowledge DESY (Hamburg, Germany), a member of the Helmholtz Association HGF, for the provisions of experimental facilities, as parts of this research were carried out at the PETRA III light source of DESY. Data was collected at P21.1 beamline operated by DESY Photon Science against proposal no. I-20221187. We would like to thank Oleh Ivashko, Ann-Christin Dippel, Martin von Zimmermann, and Philipp Glaevecke of the beamline for assistance and project administration for the experiments in DESY. The financial grant JNC/PETRA/IN-72 by the Department of Science & Technology (Government of India) for the experiments performed at DESY, provided within the framework of the India@DESY collaboration, is also gratefully acknowledged.

[1] V. Caignaert *et al.*, Phys. Rev. B **81**, 094417 (2010).
[2] V. Caignaert *et al.*, Phys. Rev. B **88**, 174403 (2013).
[3] K. Singh *et al.*, Phys. Rev. B **86**, 024410 (2012).
[4] M. Islam *et al.*, J. Magn. Magn. Mater. **529**, 167847 (2021).
[5] R. D. Johnson *et al.*, Phys. Rev. B **90**, 045129 (2014).
[6] M. v. Zimmermann *et al.*, J. Synchrotron Rad. **32**, 802 (2025).
[7] J. Rodriguez-Carvajal, *An Introduction to the Program FullProf 2000* (Laboratoire Léon Brillouin, CEA-CNRS, Saclay, France 2001).
[8] H. Hao *et al.*, Physica B **387**, 98 (2007).
[9] C. Dhanasekhar *et al.*, EPL **127**, 67001 (2019).
[10] S. Kadota *et al.*, Chem. Mater. **20**, 6378 (2008).
[11] N. Nakayama *et al.*, J. Magn. Magn. Mater. **300**, 98 (2006).
[12] M. Markina *et al.*, J. Magn. Magn. Mater. **322**, 1249 (2010).
[13] A. K. Bera *et al.*, Mater. Res. Express **2**, 026102 (2015).
[14] B. Raveau *et al.*, Comptes Rendus Chimie **21**, 952 (2018).
[15] C. Dhanasekhar *et al.*, Phys. Rev. B **96**, 134413 (2017).